STEP Team at USTC
http://space.ustc.edu.cn/dreams/

September 20, 2011, 0:25am

Critical Height for the Destabilization of Solar Prominences: Statistical Results from STEREO Observations

Kai Liu, Yuming Wang*, Chenglong Shen, and Shui Wang

CAS Key Laboratory of Geospace Environment, Department of Geophysics and Planetary Sciences, University of Science & Technology of China, Hefei, Anhui 230026, China

* *To whom correspondence should be addressed. E-mail: ymwang@ustc.edu.cn*

Contents

Abstract. At which height will a prominence inclined to be unstable, or where is the most probable critical height for the prominence destabilization? This question is statistically studied based on 362 solar limb prominences well-recognized by SLIP-CAT from 2007 April to the end of 2009. We found that there are about 71% disrupted prominences (DPs), among which about 42% of them did not erupt successfully and about 89% of them experienced a sudden destabilization (SD) process. After a comprehensive analysis of the DPs, the following findings are discovered. (1) Most DPs become unstable at the height of 0.06 – 0.14 $R_\odot$ from the solar surface, and there are two most probable critical heights, at which a prominence is much likely to get unstable; the primary one is 0.13 $R_\odot$ and the secondary one is 0.19 $R_\odot$. (2) There exists upper limit for the erupting velocity of eruptive prominences (EPs), which decreases following a power law with increasing height and mass; the kinetic energy of EPs accordingly has an upper limit too, which decreases as critical height increases. (3) Stable prominences (SPs) are generally longer and heavier than DPs, and not higher than 0.4 $R_\odot$. (4) About 62% of EPs were associated with CMEs; but there is no difference in apparent properties between EPs associated with and without CMEs.

1 Introduction

Prominences (filaments) are singularities in the corona since they consist of cool (temperature $T \leq 10^4 K$) and dense (electron density 10^9 – 10^{11} cm^{-3}) plasma in the hot and diluted coronal medium[Patsourakos and Vial, 2002]. They are sustained and confined by magnetic field lines above the chromospheres, and exhibit a strong coupling between magnetic forces and thermodynamics [Wiik et al., 1997].

When a prominence ascends with a significant velocity, it is called eruptive prominence [EP, Pettit, 1950]. As one of the earliest known forms of mass ejections from the Sun, EPs started to receive attentions since the late 1800s [See Chapter 1 in book by Tandberg-Hanssen, 1995]. Many authors have studied the relationship between EPs with coronal mass ejections (CMEs) and indicate a close association between the two phenomena [e.g., Gilbert et al., 2000; Gopalswamy et al., 2003; Schrijver et al., 2008; Filippov and Koutchmy, 2008]. House et al. [1981] suggested that the inner core of CMEs is made up of prominence material, which is believed to be the remnants of EPs. So EPs can be treated as a tracer of CMEs [Engvold, 2000], and the study of the kinematic evolution of EPs may advance our ability in prediction of the launch of CMEs.

According to Zirin [1979], prominences are inclined to erupt when their heights exceed 50 Mm. We know that the size and height of a prominence increase with age [Rompolt, 1990] and the prominence height characterizes the surrounding magnetic field [Makarov et al., 1992], which is crucial to the stability of prominences. Based on the inverse-polarity model [Kuperus and Raadu, 1974], Filippov and Den [2000] deduced that, by assuming the change of magnetic field in height a power-law function, a quiescent prominence is stable if the power index is less than unit, and will erupt when the power index becomes and exceeds unit. The magnetic field in corona at low heights is nearly homogeneous and decreases as the field of a bipole (h^{-3}) at higher heights, thus the equilibrium of a prominence would be unstable when it reaches a certain height. This height is critical for the destabilization of prominence; we call it critical height in brief. According to Filippov and Den [2000] paper, its value can be calculated by

$$h_c = -\frac{B}{dB/dh|_{h_c}} \tag{1}$$

where B is the magnetic field strength, h is the height of prominence. A follow-up study by Filippov and Zagnetko [2008] did show that prominences erupted near the heights

calculated by Eq. 1.

In this paper, we will re-exam the historical issue statistically by using the EUV 304Å data from STEREO EUVI instrument. STEREO has the so far most complete and uninterrupted observations at EUV 304Å wavelength since the late 2006. It gives us a chance to study the critical height for prominence destabilization in a statistical way with a large sample. We define that a disrupted prominence (DP) is a prominence destabilized during the period of it being detected, and a stable prominence (SP) is the prominence else. In Section 2, how we pick and classify prominences for our study is introduced. The statistical results are given in Section 3. Section 4 is designed for the conclusions and discussions.

2 Data

2.1 Selection of Prominences

Prominences above the solar limb can be clearly detected at EUV 304Å wavelength. In our previous work, a system called SLIPCAT (Solar LImb Prominence CAtcher & Tracker) had been developed to recognize and track solar limb prominences based on only He II 304Å data observed by SECCHI/EUVI onboard of STEREO. The technique of region-growing with thresholds and linear discriminant analysis are two major functions applied by SLIPCAT to recognize prominences. Lots of limb prominences as well as various parameters of each recognized prominence are obtained, and an web-based online catalog has been generated (Wang et al. 2010, hereafter Paper I). Now SLIPCAT has a complete data set for both STEREO–A and STEREO–B data from 2007 April to 2010 April (http://space.ustc.edu.cn/dreams/slipcat/).

In this paper, we will use the data set of STEREO–B from 2007 April to the end of 2009 for our study. We use STEREO–B rather than STEREO–A because STEREO–B has a larger field of view (FOV) than STEREO–A. We do not involve the data after January 2010, because the solar activity level obviously increased, and the set of calculation parameters used by SLIPCAT is different from that for the STEREO data before 2010 (refer to our website for more details).

SLIPCAT extracted 10072 'well-tracked' (see Paper I for the definition of the term) prominences based on SECCHI/EUVI 304Å data from STEREO-B during the period of interesting. Further, we narrow our sample by selecting prominences whose maximum height of leading edge from solar surface is greater than $h = 0.2$ $R_\odot$ (or 140 Mm). We believe that most prominences below 0.2 $R_\odot$ are not eruptive. A reason is that Munro et al. [1979] found that all eruptive prominences observed beyond 0.2 $R_\odot$ were associated with CMEs, which is consistent with Gilbert et al. [2000]'s study, in which it is found that all 18 EPs with a maximum height greater than 0.2 $R_\odot$ had an associated CME and only one failed to reach 0.2 $R_\odot$. Moreover, a stronger reason is given in Figure 1, which shows the distributions of the maximum height of the leading edges of SPs and DPs (the identification process of SPs and DPs is described in Sec. 2.2). For SPs, there are more event number at lower height, while for DPs, there is a peak appearing at the middle of the distribution. It indicates that the selection of 0.2 $R_\odot$ can cover most DPs.

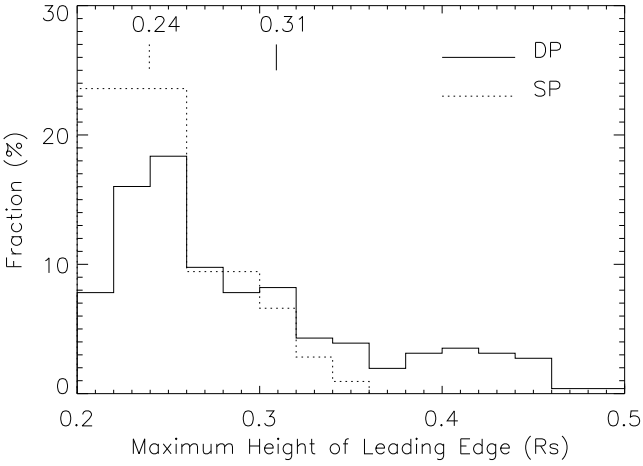

Figure 1: Distribution of the maximum height of leading edges of DPs (solid line) & SPs (dotted line). The short vertical lines with digital numbers mark the average values of histograms.

Besides, it should be noted that the prominence height obtained by SLIPCAT is projected one, and therefore is underestimated. Since prominence is an extended structure, the underestimation will be even large for some prominences locating at a significant distance away from limb. For a prominence with its top locating in 20 degrees away from limb, it could be derived that its height be underestimated by $0.06(h+1)$ $R_\odot$, which is less than 0.1 $R_\odot$ in our sample. Hence, we believe that most detected prominences should not be too far away limb, and therefore the projection effect will not significantly affect our statistical results.

2.2 Classifications of Prominences

Although almost all prominences can be recognized by SLIPCAT, however, it should be admitted that not all the recognized prominences are real prominences. Some of them are surges, and some are not well-recognized but contaminated by noise (Fig.2). Surges have a much different appearance and behavior from a typical prominence. They are relatively narrow and faint, and usually erupts quickly and radially, which means a short lifetime. By manually checking EUV 304Å movies, we remove all surges and noised prominences from our sample. Meanwhile, all the real prominences are classified into different types according to their dynamic processes during their being detected, which have been listed in Table 1.

First we classified prominences into two main types as SPs and DPs, which have been defined in the end of Sec.1. Second, DPs are classified as EPs and failure eruptive prominences (FPs). We use the definition from Gilbert et al. [2000]'s study to define an EP as one in which all or some of the prominence material appears to escape the solar gravitational field[1]. If the ascending prominence material apparently falls back down in the FOV of SECCHI/EUVI (≤ 1.7

[1]Such apparently escaping may be real, but also possibly be faked due to some thermodynamic processes (See Holly et al. 2000 and Paper I). In this paper, we do not distinguish an EP does erupt or is just heated.

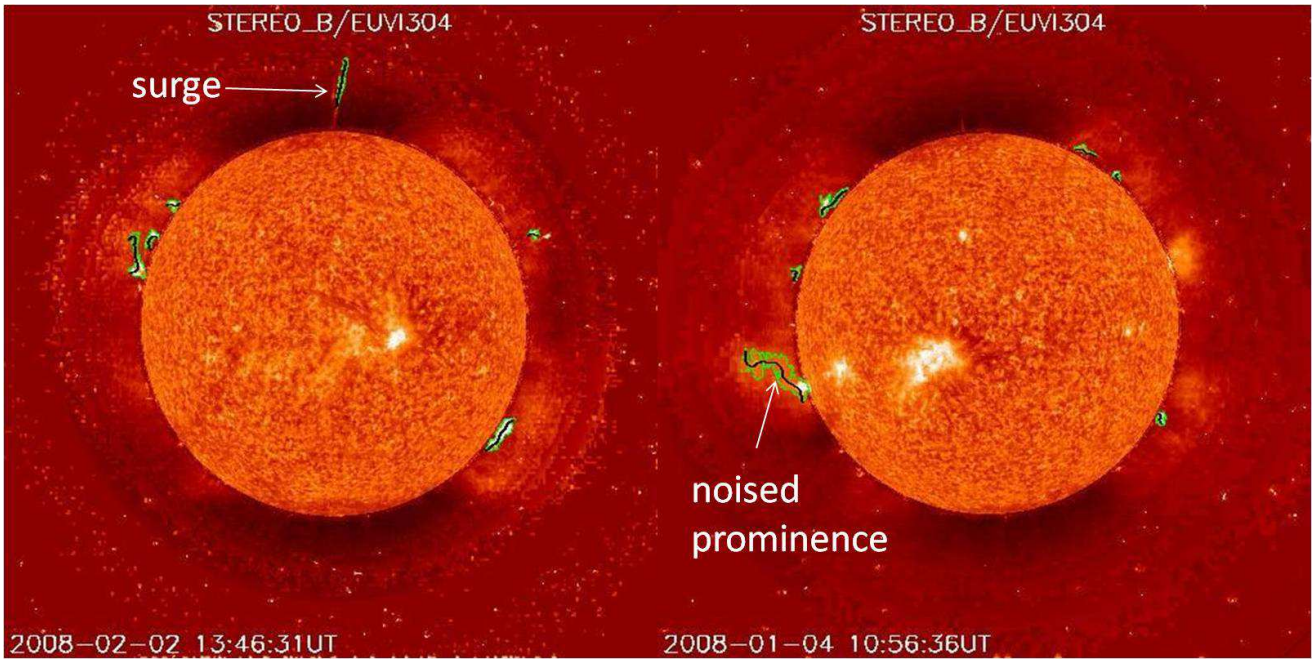

Figure 2: Example showing a surge (left) and a noised prominence (right).

$R_\odot$ for STEREO–B), we called these prominences FPs.

As an EP evolves, its leading edge may be gradual rising or experience one or multiple sudden destabilization (SD) phases. The latter means that there could be one or several points, at which the prominence get destabilization. Thus, we further divide EPs into three types. The first type is EPs with only one SD phase, which we called single-phase eruption (SE). Figure 3a–3c are three images processed by SLIPCAT showing a SE right before the eruption, during the eruption, and before it faded away around the position angle of about 218° (near the South Pole). Figure 3d gives the profile of the entire evolution process of its leading edge since 2007-06-05 03:07 UT. It is clear that there is one obvious SD point (denoted by the red arrow), before which the prominence slowly rose with a weak oscillation, and after which it was obviously suddenly accelerated to get a significant speed. The SD point just indicates the critical height of the destabilization of the prominence, and implies a catastrophic process. The erupting speed is estimated to be about 11 km/s by using a linear fitting.

Second type is more complicated. It contains EPs with multiple SD phases, which we called multiple-phase eruption (ME). Figure 4 shows an EP with position angle around 37° on 2007 June 23 for example. There are three SD points (marked in the Fig.4f as red arrows) corresponding to three SD phases in this EP's evolution process. The first and third SD phase both indicate a failed eruption, which can be seen from Figure 4a–4b and Figure 4d–4e. The second SD phase indicates a successful eruption, which is can be seen from Figure 4b–4d, and that is the reason we classified this prominence as an EP. We choose the height of the first SD point of ME as its critical height, because that is the point where the prominence loses its stability for the first time. We obtained the eruption speed of this EP by doing a linear fitting to the profile of the successful eruption phase, which is from the second SD point to the point where the escaping material is fading away, and the value is about 18 km/s.

When an EP's leading edge is rising gradually, we call it as gradual eruption (GE), which is the third type of our classification. We also give an example of GE in Figure 5. Figure 5a–5d demonstrate its appearance through fading away around position angle of 59°. Being different from the above two types, a GE does not have a SD point at all, as seeing from the evolution profile in Figure 5e. Thus, we ca not get the critical height for the destabilization of this type of EP. The ascending speed of the GE event is about 6 km/s by using a linear fit.

FPs also have one or multiple SD phases just as EPs, although the erupting materials of FPs fail down eventually according to our data, they also have critical heights for their SD phases. As same as EPs, we take the height of the first SD of a FP as its critical height. Thus, in our classification, SEs, MEs and FPs can be found a critical height where they destabilized.

In summary, there are a total of 362 well-recognized prominences with the maximum height of leading edge above 0.2 $R_\odot$ detected by STEREO–B during 2007 April – 2009 December (Table 1). In these events, there are 106 (occupying 29%) SPs during the period of detection and 256 (occupying 71%) DPs. The latter consists of 107 (42%) FPs and 149 (58%) EPs, and EPs further consist of 70 (47%) SEs, 50 (34%) MEs and 29 (19%) GEs. Besides, we list all the acronyms in the appendix for one's reference.

3 Results

3.1 Distribution of Critical Heights

The distribution of the critical heights of EPs (except GEs) and FPs, which contains 227 data points, is shown

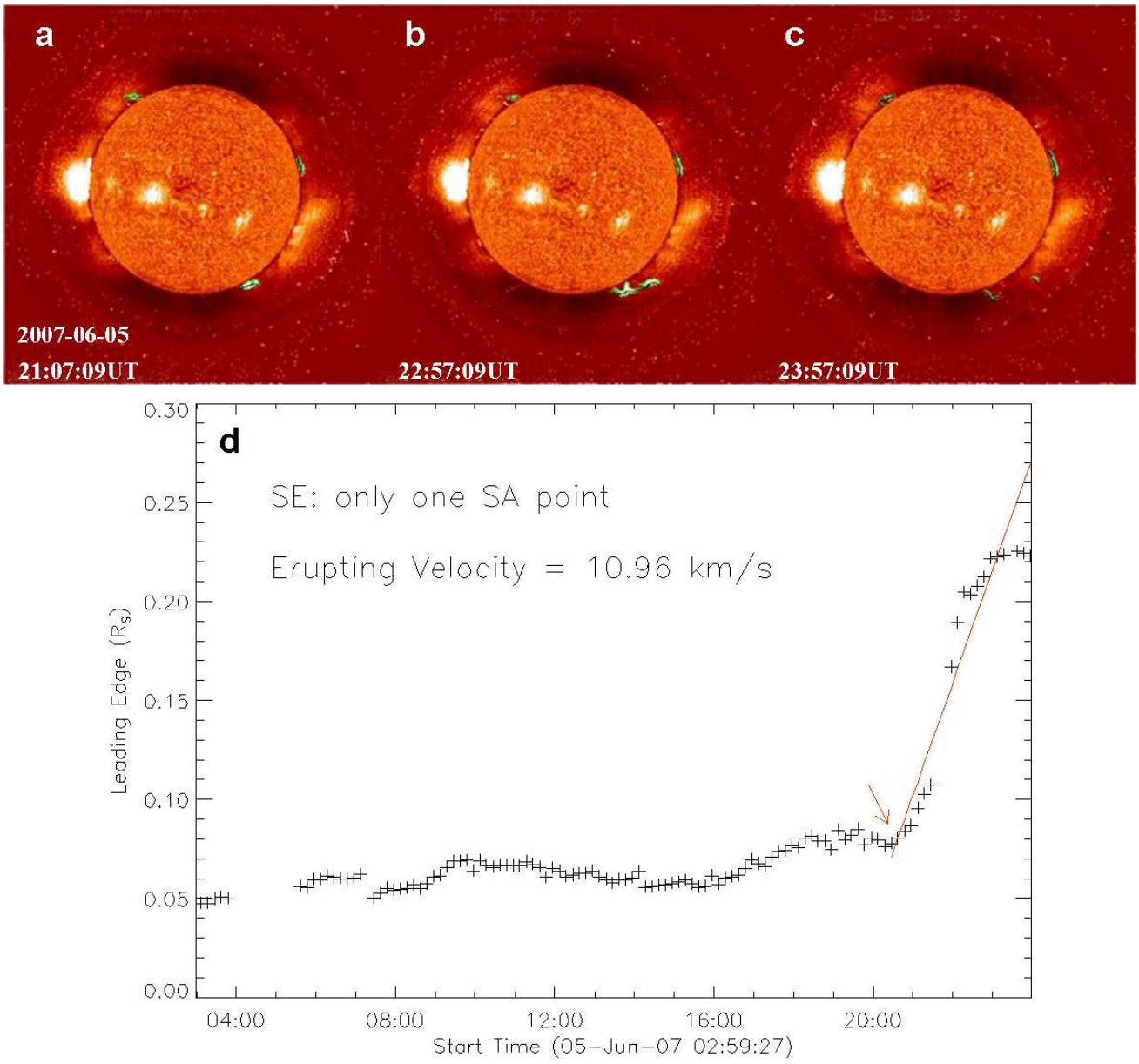

Figure 3: An example of SE.

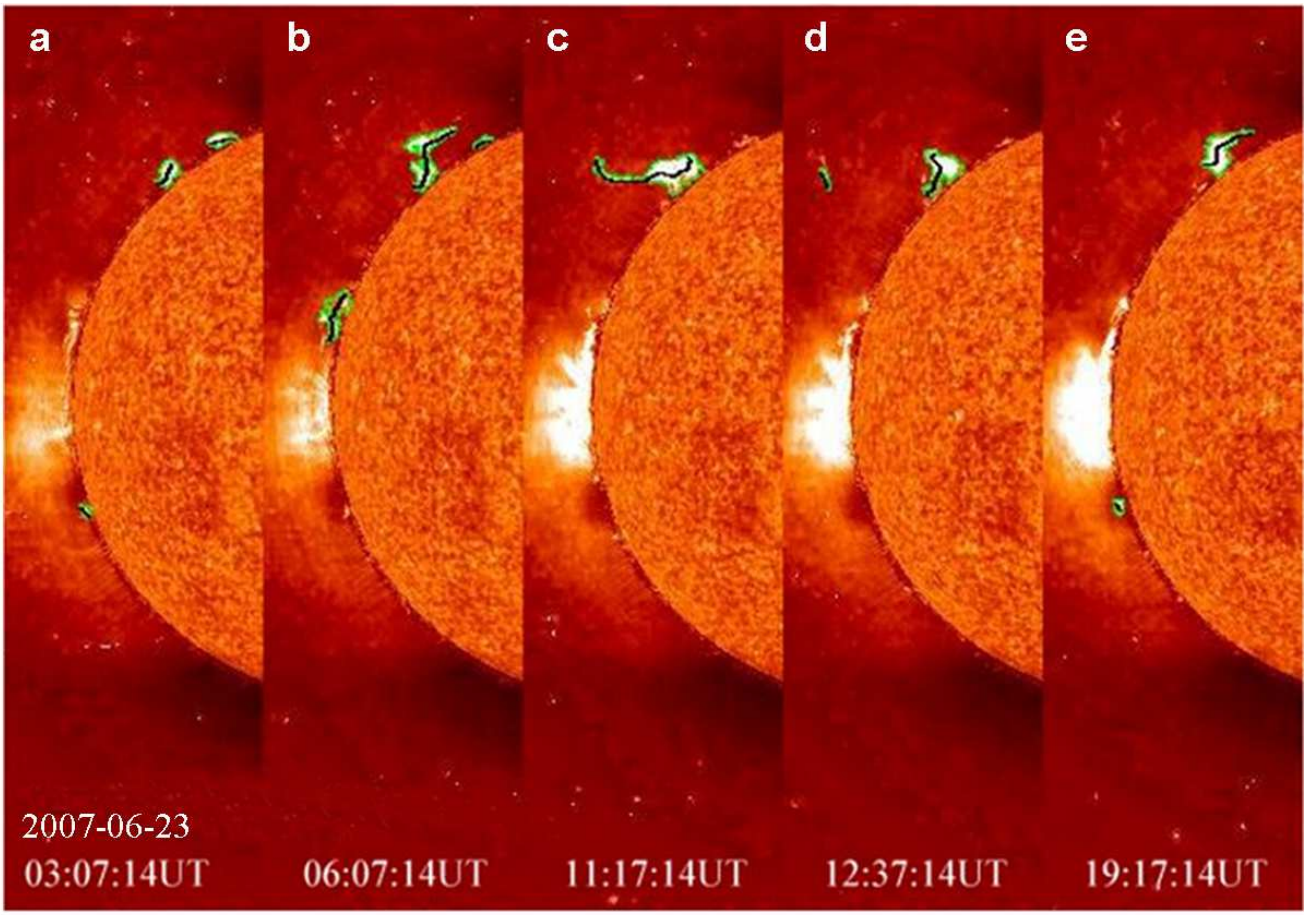

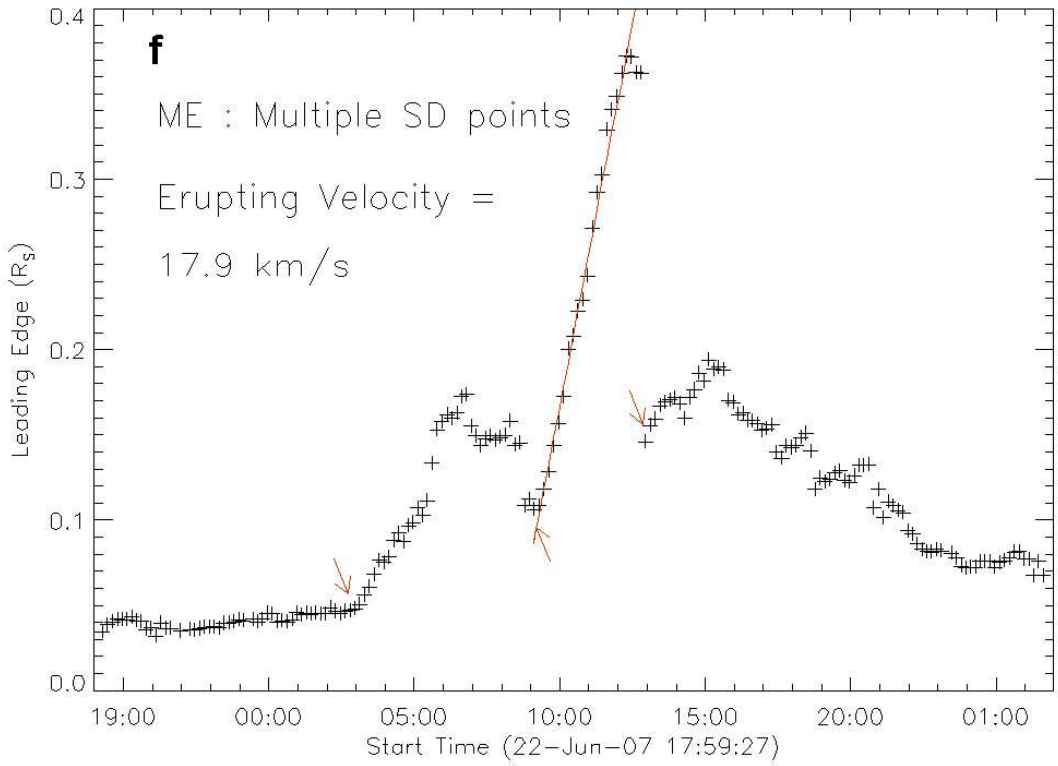

Figure 4: An example of ME.

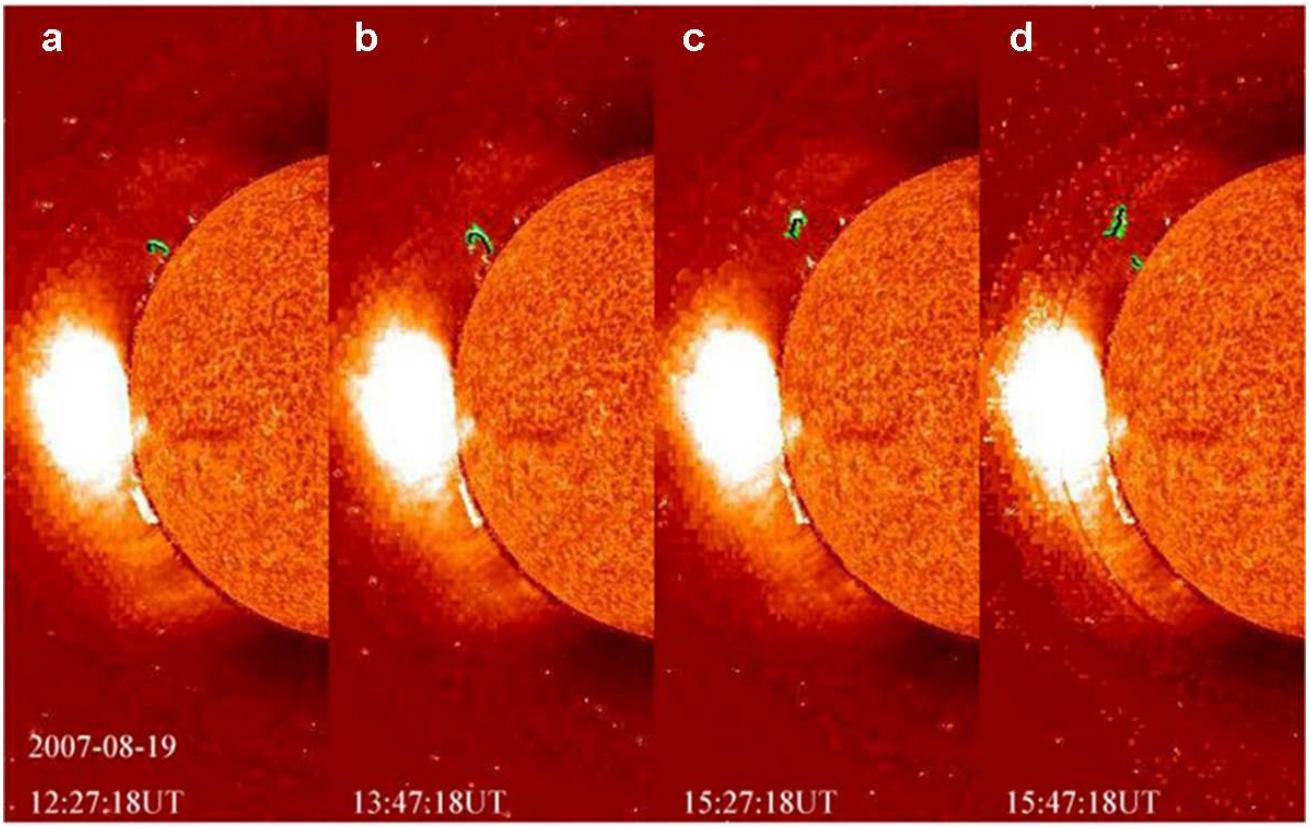

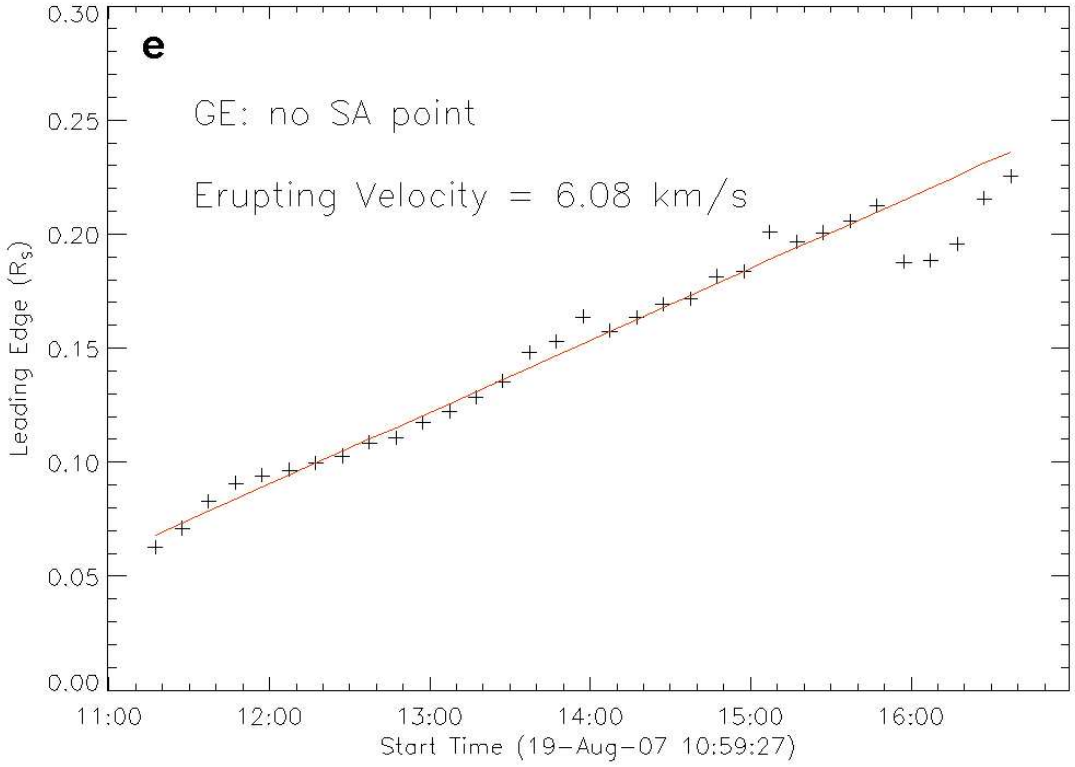

Figure 5: An example of GE.

Table 1: Classification of prominences

SPs	DPs			FPs	Total
	EPs				
	SEs	MEs	GEs		
106	70	50	29	107	362
29%	19%	14%	8%	30%	100%

in Figure 6. From the histogram, it is found that about 76% of the critical heights fall in the range of 0.06 – 0.14 $R_\odot$ with the mean value at around 0.11 $R_\odot$. Further, the asterisks connected with lines show the ratio of the number of SEs, MEs and FPs to the number of all recognized prominences by SLIPCAT (for those prominences without a critical height, the maximum height of leading edge is used). The value of the asterisk actually indicates the possibility of being unstable when a prominence reaches a certain height. The uncertainty is marked by the error bars, which calculated by the formula $\sigma = [p(1-p)/N]^{1/2}$, where p is the possibility, N is the total number of events in the bin. It should be mentioned that, the surges and noised prominences with the maximum height of leading edge larger than 0.20 $R_\odot$ are removed, but not for those smaller than 0.20 $R_\odot$. However, after a quick exam of EUVI movies, we found that most surges and noised prominences have maximum leading edge greater than 0.20 $R_\odot$ and therefore the inclusion of surges and noised prominences with the maximum leading edge lower than 0.20 $R_\odot$ will not significantly affect the values of the possibilities. The possibility distribution above the height of 0.22 $R_\odot$ is not reliable, because the event number is small and the uncertainty is significantly large. The small fraction of the events above the height of 0.22 $R_\odot$ implies that the most probable critical height will not be there. The distribution below the height of 0.22 $R_\odot$shows a double-peak feature. The two peaks appear at the height of 0.13 and 0.19 $R_\odot$, respectively. Since the first one falls in the range of 0.06 – 0.14 $R_\odot$, in which there are 76% of critical heights, we conclude that 0.13 $R_\odot$ is the primary most probable critical height and 0.19 $R_\odot$ is the secondary one.

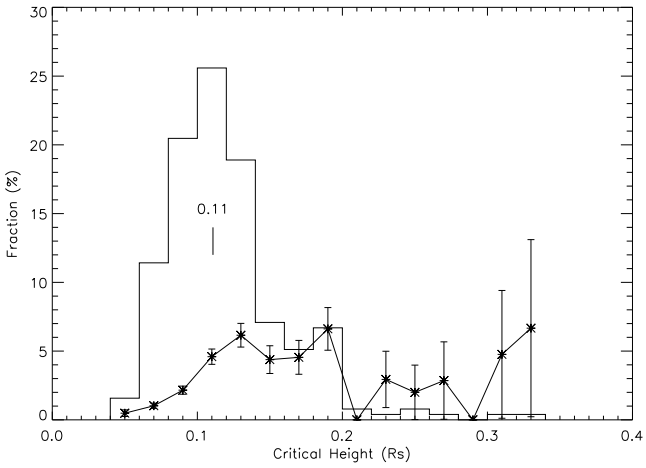

Figure 6: Distribution of critical heights (histogram) and possibilities of prominences becoming unstable at various heights (asterisks connected with lines). See main text for more details.

GEs do not have a SD point though they erupted too. Whether or not their erupting velocities are systematically different from others? This issue is inspected by comparing the distributions of the erupting velocities of GEs and the other two types of EPs (Fig.7). The average velocity of all EPs is about 14 km s^{-1}. It is found that GEs tend to have a larger erupting velocity. The result is apparently contrary to the usual physical picture that an impulsive eruption (i.e., there is a SD point) should be faster than a gradual eruption. An explanation we can have right now is that those fast GEs probably already have passed through their critical heights before they are recognized by SLIPCAT. It is possible if most of the GEs located at a significant distance away from limb. They will not be noticed until they have risen or erupted to exceed the limb.

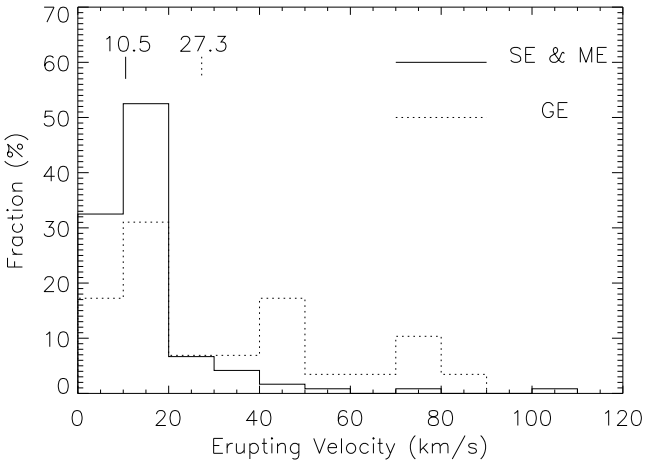

Figure 7: Distribution of EP's erupting velocity. The vertical lines with digital numbers indicate the average values.

3.2 Erupting Velocity of EPs

The comparison between the erupting velocity of GEs and the other two types of EPs has been presented in the last section. Here we will further investigate the erupting velocity of SEs and MEs and its correlations with critical height and mass. In this study, mass is approximated as the total brightness recorded by STEREO/EUVI at 304Å wavelength, and in units of digital number (DN). Scattering plots of the erupting velocity versus critical height and the erupting velocity versus mass are shown in Figure 8a and 8b. It is obvious that the maximum erupting velocity decreases with increasing critical height and mass. This result suggests that, at a certain height or for a certain mass, the kinetic energy an eruptive prominence could reach or the free magnetic energy accumulated in the prominence-related magnetic system has an upper limit.

In order to obtain the dependences of the upper limit on the height and mass, we divided the data sample into six bins as indicated by the equally-separated vertical dashed lines. The data points with erupting velocity at the top three position in each bin (marked as plus symbols) are fitted by a function $v = c_0 x^{c_1}$. For Figure 8a, x is h the critical height calculated from solar surface; for Figure 8b, x is just the mass represented by the total brightness. The fitting results

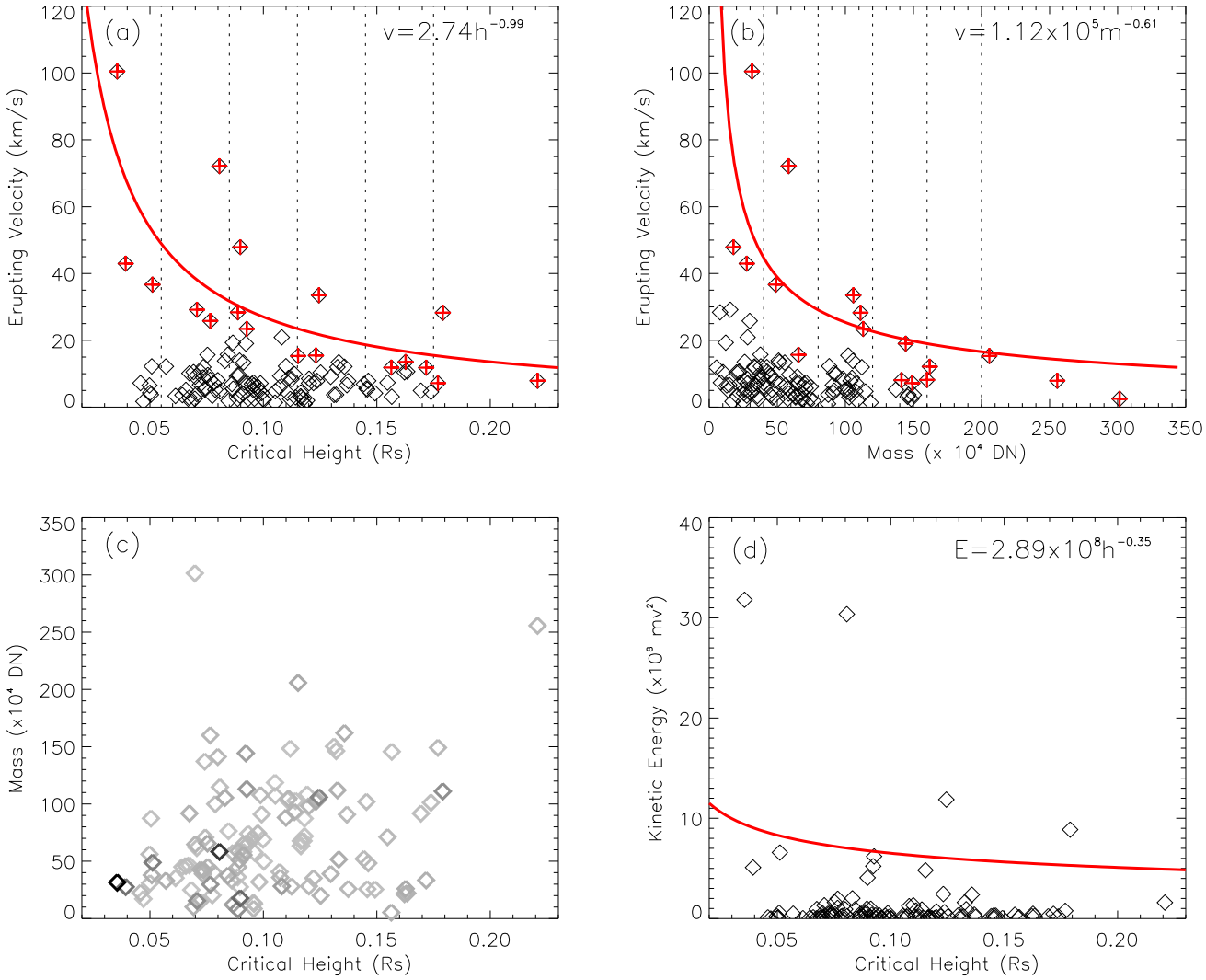

Figure 8: Correlation between (a) erupting velocity and critical height, (b) erupting velocity and mass (represented by total brightness), (c) mass and critical height, and (d) kinetic energy and critical height. In panel (a) and (b), the dashed vertical lines separate data points into 6 bins, plus symbols mark the data points having top three erupting velocity in every bin, and the solid line is the fitting curve to them, which is given by the formula at the upper right corner. In panel (c) the darker points have larger erupting velocities. In panel (d) the solid line, given by the formula at the upper right corner, is derived from the fitting functions in panel (a) and (b).

give the following two equations

$$v_{max} = 2.74h^{-0.99} \text{ (km s}^{-1}\text{)} \quad (2)$$

$$v_{max} = 1.12 \times 10^5 m^{-0.61} \text{ (km s}^{-1}\text{)} \quad (3)$$

in which h is in units of $R_\odot$ and m in units of DN. Figure 8c shows the mass versus the critical height. The darker symbol means a larger velocity. Consistent with the above results, the fast erupting prominences locate at the lower-left corner. No obvious correlation between the two parameters is revealed, which indicates that the correlations of the maximum erupting velocity with the critical height and mass are almost independent.

Further, we can derive the upper limit of kinetic energy of eruptive prominences as a function of critical height from the above fitting results as the follow equation

$$E_{max} \propto m v_{max}^2 = 2.89 \times 10^8 h^{-0.35} \text{ (DN km}^2 \text{ s}^{-2}\text{)} \quad (4)$$

The red line in Figure 8d presents the equation. Comparing it with the data points in that plot, we can find a weak consistency between them with only four data points exceeding the upper limit.

3.3 EPs vs. FPs & DPs vs. SPs

Although both EPs (except GEs) and FPs have a SD point, is there crucial difference between the properties of these two types of DPs when they go through SD point? With this question, we compared their length, area, brightness and mass at SD point, and plotted them as histograms in Figure 9. It is shown that there is no obvious difference between the two types, which indicates that one can not use these properties of a DP at SD point to decide whether or not it would have a successful eruption.

SPs do not have much change in their properties during their appearances, so we can use the mean values of the length, area, brightness and mass to present them. We compared these mean values with DPs' properties at SD point (Fig.10) to check if there is any difference. The histograms in Figure 10 show that SPs generally have a larger length, area and mass than DPs by a factor of about 1.3. It is reasonable that a large and heavy prominence tends to be stable. It is also consistent with the results obtained in the last section that a prominence with larger mass would have a smaller upper limit of erupting velocity.

3.4 CME Association of EPs

We checked the association of EPs with CMEs by using the same method as Gilbert et al. [2000]. First, we determined the position angle and eruption time of an EP of interest. Then we browsed the movies of both coronal observations from COR1 and COR2 on board STEREO–B within 2 hours of the eruption time. If there was a CME with central position angle within 30° of the position angle of the EP in either coronagraph, this EP is considered to be associated with a CME. The results are summarized in Table 2.

We find that 62% of EPs are associated with CMEs, and MEs have a relatively higher association rate than the other two types of EPs. The association rate we got is different from previous works, e.g., 94% in Gilbert et al. [2000] and 36% in Yang and Wang [2002]. The reason for these differences is mostly due to the data selection. Gilbert et al. [2000] used ground-based observations, and picked the prominences that had violent change as their objects. We believe that such a strict selection caused the high association rate. However, Yang and Wang [2002] got a much smaller association rate than others. It is because they treated prominences with transverse motion as EPs too, which are not considered in our sample. Gopalswamy et al. [2003] got an association rate of about 72%. In their work, the data from Nobeyama Radioheliograph during 1996 January – 2001 December was used to identify prominences. Their study covered the period from 1996 January – 2001 December, i.e., from solar minimum to maximum, whereas ours is near solar minimum. Thus their association rate is reasonably larger than ours because CMEs are less frequent in solar minimum than solar maximum.

Table 2: Association of EPs with CMEs

	CME-assoc./Total	Fraction
SEs	40/70	57%
MEs	35/50	70%
GEs	17/29	59%
Total	92/149	62%

We plotted distributions of EPs' critical heights and erupting velocities with (solid line) and without (dotted line) CMEs in Figure 11. They do not show much difference, which suggests that we are probably not able to forecast CMEs' occurrence based only on these properties of EPs.

Figure 11 shows that the average speed of CME-associated EPs is about 14.6 km s^{-1}, that is much lower than CME speed, which is typically hundreds kilometers per second in the outer corona. This divergence implies that prominence materials can be accelerated to considerable high speeds over one or more solar radii. The speeds measured in EUVI FOV are just initial speeds of prominence eruptions. Also the erupting speeds are much lower than the gravitational escape velocity of $\sim$ 600 km s^{-1} at the base of corona, and no obvious deceleration could be found in the velocity profiles. This suggests a continuous driving from released magnetic free energy.

4 Conclusions and Discussions

All the prominences with leading edge greater than 0.2 $R_\odot$ recognized by SLIPCAT during 2007 April – 2009 December are investigated. By manually examining the movies, these prominences are classified into various types: SP, DP, EP, FP, SE, ME and GE. The following statistical results are obtained.

1. There are about 71% DPs, about 42% of them did not erupt successfully, and about 89% of them experienced a SD process.

2. Most DPs become unstable at the height of 0.06 – 0.14 $R_\odot$. There are two most probable critical heights, at which a prominence is much likely to get unstable; the primary one is 0.13 $R_\odot$ and the secondary one is 0.19 $R_\odot$.

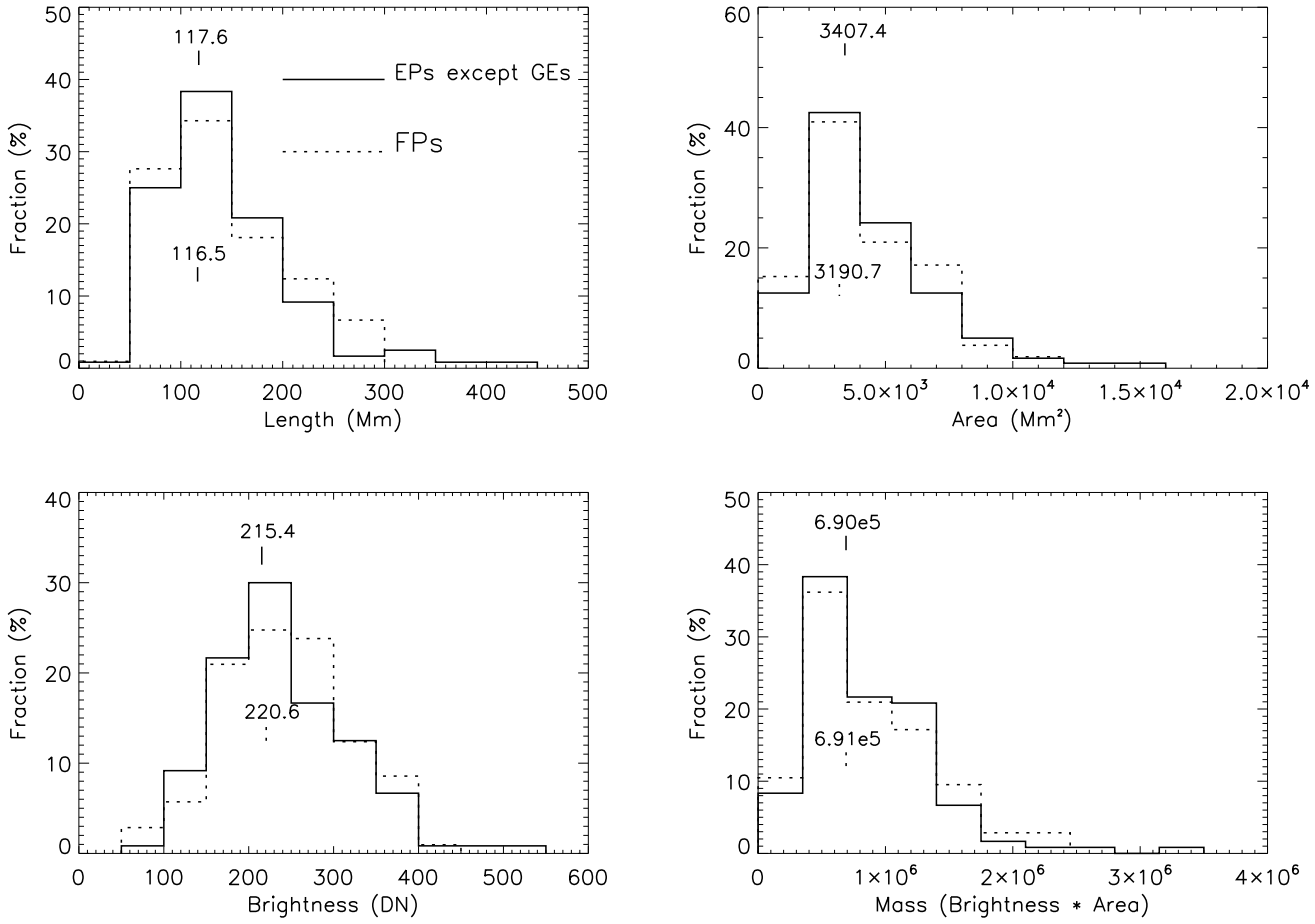

Figure 9: Distributions of the apparent properties of EPs except GEs (solid lines) and FPs (dotted lines) at SD point.

3. There exists upper limit for the erupting velocity of EPs, which decreases with increasing critical height and mass. Inferentially, the upper limit of the kinetic energy of EPs also decreases as critical height increases.

4. There is no difference in apparent properties (length, area, brightness and mass) between EPs and FPs. However, SPs are generally longer and heavier than DPs by a factor of about 1.3, and no SPs are higher than 0.4 $R_\odot$.

5. About 62% of EPs were associated with CMEs. But there is no difference in apparent properties between EPs associated with and without CMEs.

According to Eq. 1 mentioned in Sec.1, we may deduce that prominences embedded in a region with more rapid decrease in magnetic filed strength along height should have lower critical height. Thus, the primary and secondary most probable critical heights may correspond to two different types of source regions. Prominences can form in an AR or quiet Sun region. It may be the reason why there are the two most probable critical heights. To verify our conjecture, the source regions of DPs and the coronal magnetic field surrounding them must be investigated, which will be pursued in a separate paper.

Corona is dominated by magnetic field, and therefore the kinetic energy of prominences is converted from magnetic free energy. The anti-correlation of the maximum erupting velocity of EPs with the height suggests that the maximum free energy could be accumulated in a prominence-related magnetic field system is larger at low altitude than at high altitude. That means the magnetic free energy goes down as the prominence rises up or the surrounding magnetic field structure expands. Approximately, the maximum free energy when the system stays at the critical height can be related to the maximum kinetic energy of prominences, and described as

$$E_{max} = \int \frac{B_f^2}{2\mu} dx^3 \propto \overline{B}_f^2 h^3 \tag{5}$$

where $\overline{B}_f$ is the average magnetic field strength corresponding to the free energy, or approximately nonpotential component of magnetic field. In this equation, we implicitly assume that the size of the volume occupied by the magnetic field is proportional to the cubic value of critical height. Combining with the empirical formula Eq.4, one can easily derive

$$\overline{B}_f \propto h^{-1.7} \tag{6}$$

This scaling law implies that the average strength of the nonpotential component in a magnetic field structure weakens as the structure rises and expands. However, this result needs to be further justified, because Eq.4 is resulted from

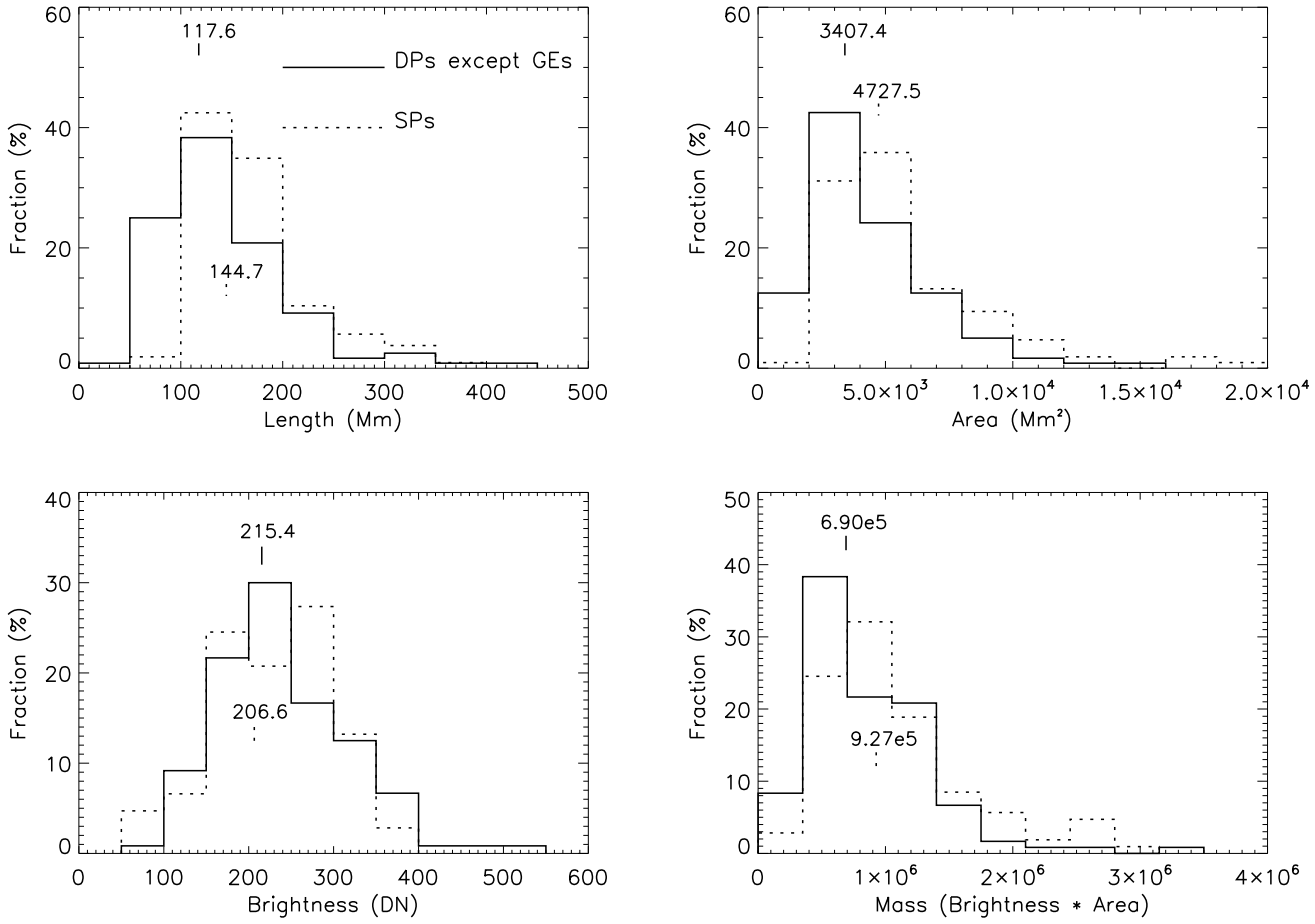

Figure 10: Distributions of the apparent properties of DPs except GEs at SD point (solid lines) and the average values of the apparent properties of SPs (dotted lines).

hundreds of events and Eq.6 is therefore established from a statistical point of view.

The manual exam of the movies gives us an impression that all the destabilization process except GEs happened within two data points. One may notice that the cadence our data is 10 minutes, which means that the catastrophic process of the prominence destabilization is shorter than 10 minutes. A question raised naturally is how quickly such a catastrophic process progresses. To answer this question and study why and how a prominence lose equilibrium, observations with higher spatial and temporal resolutions must be used. Ground-based Hα observations may be suitable for such studies, and besides, SDO provides the so far best space-borne observations that may also be able to support such studies.

Besides, the dynamic evolution of prominences can be related to the large scale structure in corona. The coronal cavities were studied by, e.g., Fuller et al. [2008] and Fuller and Gibson [2009], which are generally believed to be flux ropes supporting quiescent prominences. It was found that there were no cavities taller than 0.6 $R_\odot$. In our study, all SPs were less than 0.4 $R_\odot$ (Fig.1). The cavity flux rope is kept in equilibrium by two principle forces acting against the natural tendency for the rope to expand outward, namely, the anchored part of the field surrounding the rope, and the weight of prominence as well as the coronal helmet, [e.g., see the static model by Low and Hundhausen, 1995]. Hence, the maximum height for quiescent prominences is physically related to the maximum height of coronal cavities.

Acknowledgments. We acknowledge the use of the data from STEREO/SECCHI, and we are also grateful to the developers of SLIPCAT. We thank Dr. BC Low for his reading and valuable comments, and the anonymous referee for his/her constructive comments. This research is supported by grants from 973 key project 2011CB811403, NSFC 41131065, 40904046, 40874075 and 41121003, CAS 100-talent program, KZCX2-YW-QN511 and startup fund, FANEDD 200530, and the fundamental research funds for the central universities.

Appendix: Acronyms

AR – Active Region
CME – Coronal Mass Ejection
DN – Digital Number
DP – Disrupted Prominence
EP – Eruptive Prominence
EUVI – Extreme UltraViolet Imager
FOV – Field of View
FP – Failed Erupting Prominence
GE – Gradual Eruption
ME – Multiple Eruption
SD – Sudden Destabilization
SE – Single Eruption

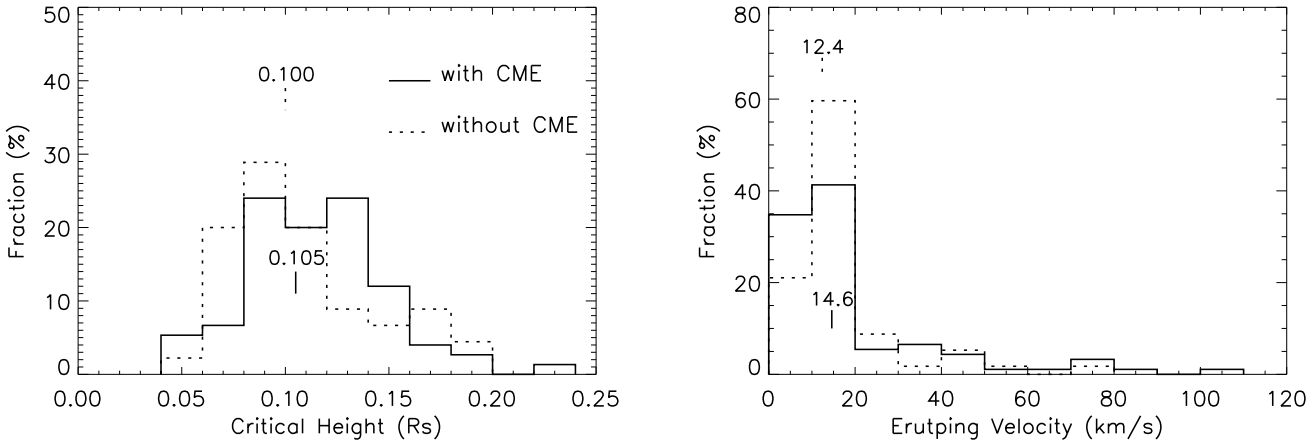

Figure 11: Distributions of critical height (left) and erupting velocity (right) of EPs with (solid lines) and without (dotted lines) CMEs.

SLIPCAT – Solar LImb Prominence CAtcher & Tracker
SP – Stable Prominence
STEREO – Solar TErrestrial RElations Observatory

References

O. Engvold. Solar prominences as a pre-eruptive state of cmes. *International Conference on Solar Eruptive Prominences*, March 2000.

B.P. Filippov and O.G. Den. Prominence height and vertical gradient in magnetic field. *Astronomy Letters*, 26:322–327, 2000.

B.P. Filippov and S. Koutchmy. Casual relationships between ertupive prominences and coronal mass ejection. *Ann.Geophys.*, 26:3025–3031, 2008.

B.P. Filippov and A. M. Zagnetko. Prominence height shows the proximity of an ejection. *JASTP*, 70:614–620, 2008.

J. Fuller and S. E. Gibson. A survey of coronal cavity density profiles. *ApJ*, 700:1205–1215, 2009.

J. Fuller, S. E. Gibson, G. de Toma, and Y. Fan. Observing the unobservable? modeling coronal cavity densities. *ApJ*, 678: 515–530, 2008.

Holly R. Gilbert, Thomas E. Holzer, Joan T. Brukerile, and Arther J. Hundhausen. Active and eruptive prominences and their relationship to coronal mass ejections. *ApJ*, 537:503–515, 2000.

N. Gopalswamy, M. Shimojo, W. Lu, S. Yashiro, K. Shibasaki, and R. A. Howard. Prominence eruptions and coronal mass ejection: a statistical study using microwave observation. *ApJ*, 586:562–578, 2003.

L.L. House, W.J. Wagner, E. Hildner, C. Sawyer, and H.U. Schmidt. Studies of the corona with the solar maximum mission coronagraph/polarimeter. *ApJ*, 244:L117, 1981.

M. Kuperus and M.A. Raadu. The support of prominences formed in neutral sheets. *Astron. Astrophys.*, 31:189, 1974.

B. C. Low and J. R. Hundhausen. Magnetostatic structures of the solar corona. 2: The magnetic topology of quiescent prominences. *ApJ*, 443:818–836, 1995.

V.I. Makarov, K.S. Tavastsherna, E.I. Davydova, and K.R. Sivaraman. Variations of prominence heights in high latitude global magnetic neutral lines. *Soln. Dannye*, 3:90–97, 1992.

R.H. Munro, J.T. Gosling, E. Hildner, R.M. MacQueen, A.I. Poland, and C.L. Ross. The association of coronal mass ejection transients with other forms of solar activity. *Sol. Phys.*, 61:201, 1979.

Spiros Patsourakos and Jean-Claude Vial. Soho contribution to prominence science. *Sol. Phys.*, 208(2):253–281, 2002.

E. Pettit. The evidence for tornado prominences. *PASP*, 62:144, 1950.

B. Rompolt. Small scale structure and dynamics of prominences. *Hvar Obs. Bull.*, 14:37–102, 1990.

Carolus J. Schrijver, Christopher Elmore, Bernhard Kliem, Tibor Török, and Alan M. Trrle. Observations and modeling of the early acceleration phase of erupting filaments involved in coronal mass ejections. *ApJ*, 674:586–595, 2008.

E. Tandberg-Hanssen. *The Nature of Solar Prominences*. Kluwer Academic, Dordrecht, 1995.

Yuming Wang, Hao Cao, Junhong Chen, Tengfei Zhang, Sijie Yu, Huinan Zheng, Chenglong Shen, Jie Zhang, and S. Wang. Solar limb prominence catcher & tracker (slipcat): An automated system and its preliminary statistical results. *ApJ*, 717(2):973–986, 2010.

J.E. Wiik, B. Schmieder, T. Kucera, A. Poland, P. Brekke, and G. Simnett. Eruptive prominence and associated cme observed with sumer, cds and lasco (soho). *Sol. Phys.*, 175(2):411–436, 1997.

G. Yang and Y. Wang. Statistical studies of filament disappearances and cmes. In Magnetic Activity and Space Environment, Proc. COSPAR Colloq., editors, *H.N. Wang and R.L. Xu*, 14, page 113, Boston pergamom, 2002.

H. Zirin. *The ecology of prominences*, volume Proceeding of the IAU Colloquium 44 of *in Physics of Solar Prominences*. Int. Astron. Union, Paris, 1979.